Photometric Compensation to Dynamic Surfaces in a Projector-Camera System

Panagiotis-Alexandros Bokaris[1(✉)], Michèle Gouiffès[1], Christian Jacquemin[1], and Jean-Marc Chomaz[2]

[1] LIMSI-CNRS, University of Paris-Sud, 91405 Orsay Cedex, France
bokaris@limsi.fr
[2] LadHyX, CNRS, École Polytechnique, 91128 Palaiseau, France

Abstract. In this paper, a novel approach that allows color compensated projection on an arbitrary surface is presented. Assuming that the geometry of the surface is known, this method can be used in dynamic environments, where the surface color is not static. A simple calibration process is performed offline and only a single input image under reference illumination is sufficient for the estimation of the compensation. The system can recover the reflectance of the surface pixel-wise and provide an accurate photometric compensation to minimize the visibility of the projection surface. The color matching between the desired appearance of the projected image and the projection on the surface is performed in the device-independent color space CIE 1931 XYZ. The results of the evaluation confirm that this method provides a robust and accurate compensation even for surfaces with saturated colors and high spatial frequency patterns. This promising method can be the cornerstone of a real time projector-camera system for dynamic scenes.

Keywords: Photometric compensation · Dynamic surface · Projector-camera system · Augmented reality · Reflectance estimation · Calibration

1 Introduction

The emerging technology of projector-camera systems is used in a wide range of applications such as augmented reality, education, cultural heritage and interactive art installations. The ability to project on arbitrary surfaces expands the limits of common multimedia and breaks new ground in human-computer interaction. Over the last decade, a significant amount of research has been done in the field of smart projection and various methods have been proposed for photometric and geometric compensation in projector-camera systems. However, a system that is able to compensate for complex dynamic surfaces still remains an open issue. The main reason is that the compensation of such a system highly depends on the projection surface. Thus, the majority of the proposed methods calibrate the system for a given surface. If the surface is not static, then the

L. Agapito et al. (Eds.): ECCV 2014 Workshops, Part III, LNCS 8927, pp. 283–296, 2015.
DOI: 10.1007/978-3-319-16199-0_20

system has to be recalibrated for the new surface. This leads to solutions that cannot be applied in real time and cannot handle a dynamic environment.

In general, the physical characterization of a surface requires to measure its spectral reflectance. However, obtaining such spectral data requires the use of special equipment such as a spectrophotometer or a spectral camera. This is not feasible in the majority of applications and, in addition, it is impractical to perform a significant amount of measurements for each surface.

The main contribution of this work is a robust and accurate photometric projector compensation method that can be adapted to changes on the projection surface. For this purpose, we propose a novel calibration method that does not require the projection of any calibration pattern and is entirely performed offline. Once, the system is calibrated, a single input image of the projection surface under reference illumination is sufficient for estimating the compensation. The offline calibration consists of two different procedures. The first one is to build the surface reflectance estimator using a small training set and least square data fitting. For the training set, pairs of RGB camera values and spectral reflectances are required. Thus, capturing, with the camera, a single image of a surface that has color patches with known reflectances is sufficient. The second procedure requires the measurement of the spectral responses of the RGB projector primaries. If this is not provided by the manufacturer, it can be easily obtained using a spectroradiometer. Despite requiring the use of special equipment, it has the main advantage that it is performed only once for each projector.

Once the offline calibration is achieved, the proposed method performs the color matching between the desired appearance of the projected image and the result of the projection on the surface in the independent color space CIE 1931 XYZ. Using the estimated surface spectral reflectance, the RGB values of the projector that would produce the desired image appearance are calculated.

It should be noted that since this paper focuses on the photometric compensation, it is assumed that the camera-projector correspondence has been already performed as a pre-processing step. The geometric compensation is a well studied problem. For the purposes of this research, the structured light technique proposed in [18] and applied in [12] was used for the mapping between the projector and camera pixels.

2 Previous Work

There is an increasing interest in the projector-camera systems due to their wide application range. Therefore, over the last decade, numerous methods for photometric and geometric compensation have been proposed in the literature. These methods can be separated by whether they consider the projection surface static or dynamic.

Nayar et al. [13] proposed a compensation method which is based on an offline calibration that estimates the parameters of their radiometric model. The main drawback of this method is that it requires the projection of 260 images and the a priori knowledge of the camera's response function. Grossberg et al. [7] improved

this radiometric model and presented a calibration process that requires the projection of only 6 images. Even though this method provides promising results, it is only applicable in static environments since every time the projection surface changes, the projection of the calibration images has to be repeated. Bimber et al. [4] introduced the concept of smart projectors which use cameras to capture information about the environment. They provide a compensation method for projecting on arbitrary surfaces. However, their rather simple radiometrical model is not able to compensate for the complex nonlinearities in a projector or camera.

Ashdown et al. [3] proposed a compensation method that is content-dependent. The compensation image is calculated according to the values of chrominance and luminance that the system can produce. In other words, the desired appearance is fitted to the available gamut. However, CIELUV was used as the perceptually-uniform color space, which is well-known for its poor uniformity. Moreover, this approach requires a set of calibration images for each surface. Law et al. [9] introduced a perceptually based method for modifying the appearance of a surface. In their work, the physical surface is separated into patches of uniform color and an optimization process computes the compliant appearance which is the most perceptually similar to the desired appearance. This approach requires the surface to be composed of uniform color patches and has a considerably high time complexity that can be up to one hour for a complex scene.

Recently, Grundhofer [8] proposed a method that does not require projector or camera calibration. The pixel-wise mapping from projector to camera colors is generated by a sparse sampling of the projector's color gamut and a scattered data interpolation. In addition, an optional offline optimization step scales locally the input image, maximizing the achievable luminance and contrast while still preserving smooth input gradients, in order to avoid out-of-gamut artifacts. One of the main disadvantages of this approach is that it requires a considerably big set of images (125) in order to perform the necessary color mapping.

A different approach to photometric compensation is based on the acquisition of the light transport instead of projecting calibration images ([17], [14]). The use of the inverse light transport provides new possibilities for analyzing and canceling complex effects such as interreflections that cannot be compensated in a traditional photometric compensation. However, obtaining the light transport of the scene is a highly time-demanding operation that can take more than one hour. In addition, the time complexity of inverting the light transport is another constraint that limits the method to static scenes.

Besides the aforementioned methods that are limited to static surfaces, there are some methods proposed in the literature that can handle dynamic surfaces. Fujii et al. [6] presented a coaxial projector-camera system in order to avoid the problem of continuous geometrical mapping in a moving environment. Their radiometric model is similar with the one in [7] and the system can adapt to a moving surface by capturing a single frame instead of performing full recalibration. However, in order to achieve this, the surface reflectance is treated as a

constant within each camera band. This is a very strong assumption and it is not valid for the majority of surface colors. Furthermore, the nonlinearities in projector and camera responses are considered to be negligible and the authors suggest an extra pre-calibration of the devices in order to be taken into account. Amano and Kato [2] introduced a coaxial system that uses a model prediction controller in order to change the appearance of a surface and was later expanded in [1]. This method requires a calibration procedure and the reflectance estimation suffers the same constraints as in [6]. Moreover, due to the use of the controller, the output requires several frames in order to be stabilized.

Park et al. [15] followed a different approach and introduced a system that continuously projects a special embedded pattern image, which allows the radiometric and geometric compensation on a dynamic surface. The embedded information used for the compensation can be encoded in the pattern either temporally or spatially. As a result, there is a tradeoff in this method between the information that can be hidden in the embedded pattern and the visibility of the pattern. Unfortunately, according to their results, the compensation starts to become acceptable only when the pattern can be perceived by the viewer.

3 Methodology

In Section 3.1, the photometric model proposed in this paper is presented. Then, the calibration procedure of the system is separated in two parts. The first one (Section 3.2) is to build the surface reflectance estimator that takes a single camera image as an input. The second part (Section 3.3) describes the linearization and calibration of the devices. Finally, once the calibration procedure has been performed offline, the compensation image can be computed online as described in Section 3.4.

3.1 Photometric Model

As it is well known, the camera and the projector are devices with non-linear responses. In a digital camera the relation between the RGB values and the illuminance impinging on its sensor, can be adequately described by a gamma function. Thus, the RGB values of the camera have to be linearized before any transformation in a linear color space, such as CIE 1931 XYZ, is performed.

$$E_c = \alpha_c \left(C_c\right)^{\gamma} + \beta_c \tag{1}$$

where E_c is the measured illuminance, C_c the camera color channel, α_c is a scalar that simulates the gain in the camera and β_c represents the offset due to noise. The subscript c denotes a single camera channel. Each camera channel should be addressed individually since the gain is not always identical in each channel.

The non-linear response of a projector is, usually, more complex and cannot be represented by a gamma function. However, since it is still monotonically increasing by increasing channel value, it can be inverted. The relation between

the channel input value C_p and the corresponding output luminance $L_p(\lambda)$ emitted by the projector can be represented by a non-linear function $p_p()$. The result is modulated by the spectral response $q_p(\lambda)$ that is unique for each primary of the projector. The subscript p denotes a single projector channel.

$$L_p(\lambda) = p_p\left(C_p\right) q_p(\lambda) \tag{2}$$

where λ is the wavelength in the visible range of the spectrum.

The spectral illuminance $I(\lambda)$ that is reflected by a single point on the projection surface towards the direction of the camera can be formulated as follows:

$$I(\lambda) = \left(L(\lambda) + S(\lambda)\right) r(\lambda) \tag{3}$$

where $L(\lambda)$ is the total luminance emitted by the projector, $S(\lambda)$ is the luminance of the ambient light in the room and $r(\lambda)$ is the spectral reflectance of the surface point.

The illuminance, E_c in (1), measured by the camera, which has a spectral response for each channel $q_c(\lambda)$, is given by:

$$E_c = \int \left(L(\lambda) + S(\lambda)\right) r(\lambda)\ q_c(\lambda)\ d\lambda \tag{4}$$

Instead of working with the device-dependent digital values provided by the camera, as it is usually done in the literature ([13], [7], [6], [15]), we choose to perform the appearance matching in the device-independent color space CIE 1931 XYZ. By doing so, the matching becomes more accurate and the system more flexible since it is easier to replace the camera with another one. Therefore, the reflected illuminance of a point on the projection surface is described by its XYZ values. In other words, the spectral response of the camera is replaced by the CIE 1931 2^o Standard Observer as follows:

$$X = \int_{380nm}^{780nm} \left(L(\lambda) + S(\lambda)\right) r(\lambda)\ \bar{x}(\lambda)\ d\lambda \tag{5}$$

where $\bar{x}(\lambda)$ is one of the three CIE color matching functions. In a similar way as (5), Y and Z are given for $\bar{y}(\lambda)$ and $\bar{z}(\lambda)$, respectively.

3.2 Reflectance Estimation

As can be seen in (5), it is essential to know the spectral reflectance of the surface in order to calculate the XYZ values of the light reflected on it. Since this information is not provided, we propose a reflectance estimator that takes as an input a single camera image. All the below procedure is performed pixel-wise.

Assuming that $\{\lambda_t\}_{t=1}^{81}$ are uniformly spaced wavelengths in the interval [380, 780] nm, the camera response of (4) can be expressed in its discrete form as:

$$\left(x_1 x_2 x_3\right)^T = x \approx W_L^T r \tag{6}$$

where $r = (r(\lambda_1), \ldots, r(\lambda_{81}))^T \in \mathbb{R}^{81\times 1}$ is the discrete spectral reflectance, $W_L = LW \in \mathbb{R}^{81\times 3}$ corresponds to light source weighted response functions, $L \in \mathbb{R}^{81\times 81}$ is the diagonal matrix formed by the illumination vector of the total light impinging on the surface $l = (l(\lambda_1), \ldots, l(\lambda_{81}))^T$ and $W = [s_1 s_2 s_3] \in \mathbb{R}^{81\times 3}$ is the matrix of the camera responses, where $s_c = (s_c(\lambda_1), \ldots, s_c(\lambda_{81}))^T$ is the response function of each channel.

The aim of this section is to build a reflectance estimator using a training set and least squares data fitting. Let $x \in \mathbb{R}^k$ be a sensor measurement corresponding to a known spectral reflectance $r \in \mathbb{R}^n$. In our case, $k = 3$ and $n = 81$. The training set composed of m different reflectances is:

$$\{(x_1, r_1), \ldots, (x_m, r_m)\} \subset \mathbb{R}^k \times \mathbb{R}^n \tag{7}$$

The least squares minimization problem that minimizes the empirical loss can be written as:

$$\underset{C_r \in \mathbb{R}^{n\times N}}{\operatorname{argmin}} \sum_{i=1}^{m} \left\| \Phi(X) C_r^T - M \right\|_F^2 \tag{8}$$

where $\|.\|_F$ denotes Frobenius norm and the rows of matrix M contain the m reflectance vectors of the training set $M = [r_1 \ldots r_m]^T \in \mathbb{R}^{m\times n}$. $\Phi(X) = [\Phi(x_1) \ldots \Phi(x_m)]^T \in \mathbb{R}^{m\times N}$ is the feature map of N features and the solution C_r can be now written as:

$$C_r^T = \left(\Phi(X)^T \Phi(X)\right)^{-1} \Phi(X) M \tag{9}$$

The estimation of the reflectance is provided by the following equation:

$$\hat{r} = C_r \Phi(x)^T \tag{10}$$

A third degree feature map was selected for fitting the data since through our experimentation it was found that it provides the most accurate results without over-fitting the data. Feature maps of up to fourth degree were tested.

$$\begin{aligned} \Phi(X) = (&1, x_1, x_2, x_3, x_1^2, x_2^2, x_3^2, x_1x_2, x_1x_3, x_2x_3, \\ &x_1^3, x_2^3, x_3^3, x_1x_2x_3, x_1^2x_2, x_1^2x_3, x_2^2x_1, x_2^2x_3, x_3^2x_1, x_3^2x_2)^T \end{aligned} \tag{11}$$

The training set for the reflectance estimator can be easily obtained by capturing an image of a surface that is composed of m uniform patches with known reflectance under reference illumination. The patches ideally should be Lambertian but small specularities do not affect significantly the compensation, as can be seen in the results.

3.3 Device Characterization

The characterization of a projector requires spectroradiometric or colorimetric measurements of the light emitted by the device. In order the RGB-to-XYZ

transformation and the nonlinear transfer function for each primary color channel to be derived, a color ramp should be measured separately for each primary color channel. Using a spectroradiometer and measuring the radiance emitted by the device while increasing the value of each channel separately, one can obtain the spectral responses of Fig. 1(a). This figure shows the output of the projector given by (2), which consists of the spectral response of each channel weighted by a factor. As illustrated in Fig. 1(b), this weighting factor is not linear.

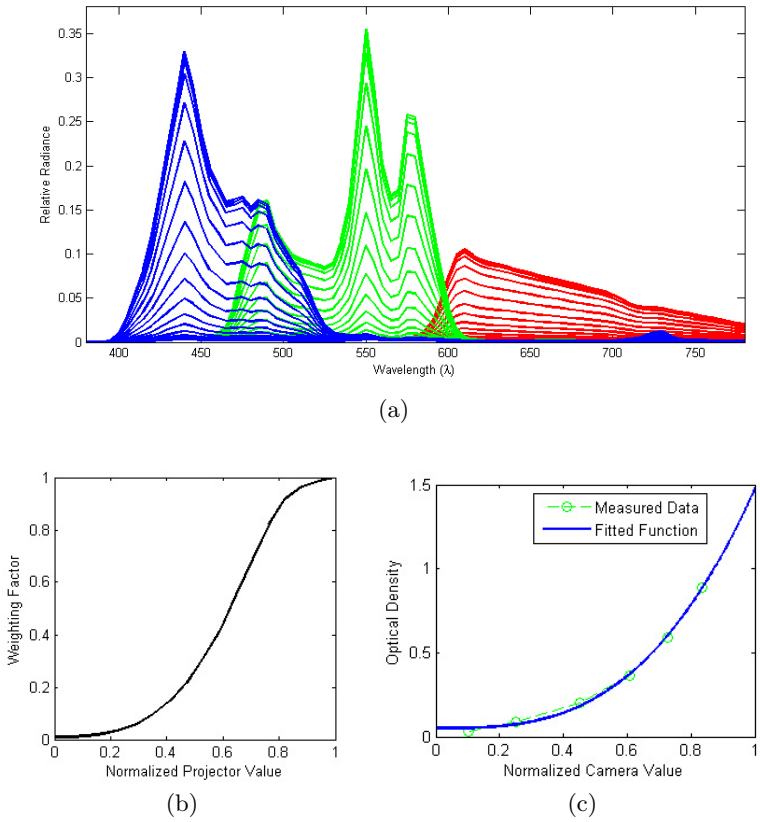

Fig. 1. (a) The spectral radiance emitted by a projector while increasing the input value of each channel individually. With blue, green and red is marked the radiance of the corresponding color channel. (b) The non-linear function of the weighting factor with respect to the projector channel value. (c) The gamma response function of the camera.

The nonlinearity of the camera can be estimated by acquiring an image of a target, such as the Macbeth ColorChecker [11], which has surfaces of varying optical density, under reference illumination. By plotting the optical density as

a function of the camera values, the gamma function of the camera, as it is expressed in (1), can be derived (see Fig. 1(c)).

3.4 Photometric Compensation

The photometric compensation should create an image that once projected on the surface would produce the desired appearance. The device-dependent RGB values of the projector and the camera should be transformed to a device-independent color space in order to make this match feasible. In this work, the CIE 1931 XYZ color space was selected. Thus, the reference camera image should be transformed to the CIE XYZ color space. Since this is a linear transformation the RGB values of the image should be first linearized by taking into account the gamma function that was obtained during the camera characterization. Then, the transformation can be performed by using a linear transformation matrix M that depends on the reference illumination of the projector.

$$\begin{bmatrix} X \\ Y \\ Z \end{bmatrix} = M \begin{bmatrix} R_{linear} \\ G_{linear} \\ B_{linear} \end{bmatrix} \tag{12}$$

In case the sRGB model is assumed for the reference image, a common transformation matrix M that corresponds to the illuminant D65 can be used:

$$M = \begin{bmatrix} 0.4124 & 0.3576 & 0.1805 \\ 0.2126 & 0.7152 & 0.0722 \\ 0.0193 & 0.1192 & 0.9502 \end{bmatrix} \tag{13}$$

However, under this assumption, the XYZ values obtained should be transformed to the corresponding XYZ values under the reference illumination of the projector, using a color constancy transform, such as CAT02 [5].

The light emitted by the projector can be approximated by the sum of its individual primaries. Even though this additivity property requires the independence of the projector's color channels, it provides an adequate estimation of the projector's output, as can be seen in our results. Thus, the total light emitted by the projector can be formulated as follows:

$$E(\lambda) = a\ q_r(\lambda) + b\ q_g(\lambda) + c\ q_b(\lambda) \tag{14}$$

where $q_r(\lambda)$, $q_g(\lambda)$ and $q_b(\lambda)$ are the spectral responses of the color channels of the projector and a, b and c their weighting factors that depend on the input value (see Fig. 1(b)).

Taking into account (14) and (5), the XYZ values of the projector on the projection surface are given by:

$$X = \int_{380nm}^{780nm} (a\ q_r(\lambda) + b\ q_g(\lambda) + c\ q_b(\lambda))\, r(\lambda)\ \bar{x}(\lambda)\ d\lambda \tag{15}$$

Y and Z are similarly given for $\bar{y}(\lambda)$ and $\bar{z}(\lambda)$, respectively. Once the surface reflectance $r(\lambda)$ is estimated and the desired $XYZ_{desired}$ values of the reference images are calculated, the emitted light of the projector that would produce the same XYZ values is computed. According to (15) it is sufficient to estimate the weighting factors of (14) since the spectral responses of the primaries are known. The ambient light of the room $S(\lambda)$ is considered negligible but it can be taken into account in case it is measured.

Matching the above XYZ values with the desired ones leads to the following 3×3 system:

$$\begin{bmatrix} a \\ b \\ c \end{bmatrix} = \begin{bmatrix} X_r & X_g & X_b \\ Y_r & Y_g & Y_b \\ Z_r & Z_g & Z_b \end{bmatrix}^{-1} \begin{bmatrix} X_{desired} \\ Y_{desired} \\ Z_{desired} \end{bmatrix} \tag{16}$$

where

$$X_c = \int_{380nm}^{780nm} q_c(\lambda) r(\lambda) \bar{x}(\lambda) d\lambda \tag{17}$$

and $c = r, g, b$. Y_c and Z_c are similarly given for $\bar{y}(\lambda)$ and $\bar{z}(\lambda)$, respectively.

4 Experimental Results

After describing the details of the calibration process, some of the achieved compensations on demanding surfaces are illustrated. Finally, the quantitative evaluation of the results is concluding this section.

4.1 Characterization

The camera-projector system that was used in this paper is composed of a Nikon D90 dSLR camera and a DLP projector Christie F1+. The resolution of the camera was set to 2144×1424 pixels while the resolution of the projector was set to its nominal 1400×1050 pixels. Even though the available single-chip DLP projector has a considerably complex characterization process [16] and the channel additivity assumption does not stand completely for this projector as can be seen in Fig. 2(a), the compensation results presented in the following section state that the proposed model can still describe the system.

For the characterization of the devices, a Minolta CS-1000 spectroadiometer was used. The projector was characterized by measuring the emitted radiance for 18 uniformly distributed values in each color channel (Fig. 1(a)).

The reflectance estimator was built using the patches of the ColorChecker and 18 different uniform color sheets that were captured by the camera and their reflectances were measured by the spectroradiometer. Using only the 24 samples of the ColorChecker was not sufficient for providing accurate reflectance estimation in a wide variety of projection surfaces. However, by simply adding 18

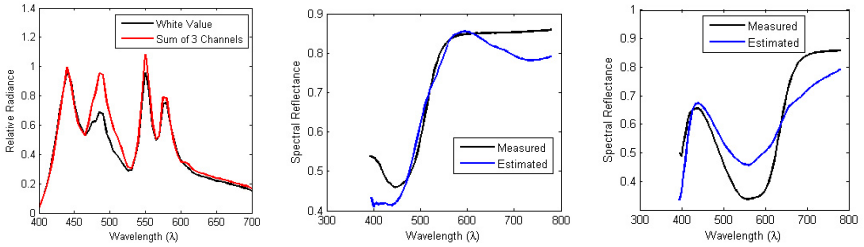

(a) (b) (c)

Fig. 2. (a) The spectral relative radiance of the white color and the sum of the individual color channels.(b) Estimated and measured reflectance of yellow patch. (c) Estimated and measured reflectance of purple patch.

additional patches, this small training set (42 pairs in total) was sufficient to provide accurate compensations even for surfaces with colors that were not included in the training set, as can be seen in the results. It should be noted that some specularities that were present in the color sheets do not affect dramatically the result. In order to evaluate the reflectance estimation, the reflectances of the color patches on the first surface in Fig. 4 were measured. The results for the yellow and the purple patch are shown in Figs. 2(b) and Fig. 2(c). Their corresponding CIE 2000 color difference [10] ΔE_{00} between the measured and estimated reflectance under the illuminant D65 was 1.64 and 8.24 units, respectively. Obviously, the reflectance of the surface cannot be considered constant within each projector and camera band as assumed in [6] and even small spectral differences introduce perceptible errors.

4.2 Compensations

A common problem while projecting on an arbitrary surface is that some colors of the initial image might not be reproducible. Thus, in the literature the majority of the proposed methods perform compensations on surfaces that are not saturated and the transition from one color to the next is very smooth because the human visual system is less sensitive to such low spatial frequencies. However, one of the goals of this paper is to compensate for complex surfaces without significantly constraining their context. In Fig. 4 (first row, first column), a surface that is composed by many colorful patches with strong edges and the resulting compensation for two different input images is presented. The compensation was tested on two images of characteristic difficulty. The first one is very vivid while the second one quite achromatic and of high contrast (see Fig. 3).

In case the projection surface moves or changes (e.g. moving object/projector) the compensation breaks and introduces dramatic artifacts even for a small displacement of the projection surface. The proposed method can adapt to the new surface by only capturing a new image under the reference illumination of the

Fig. 3. The image 1 (left) and the image 2 (right) projected on a white surface

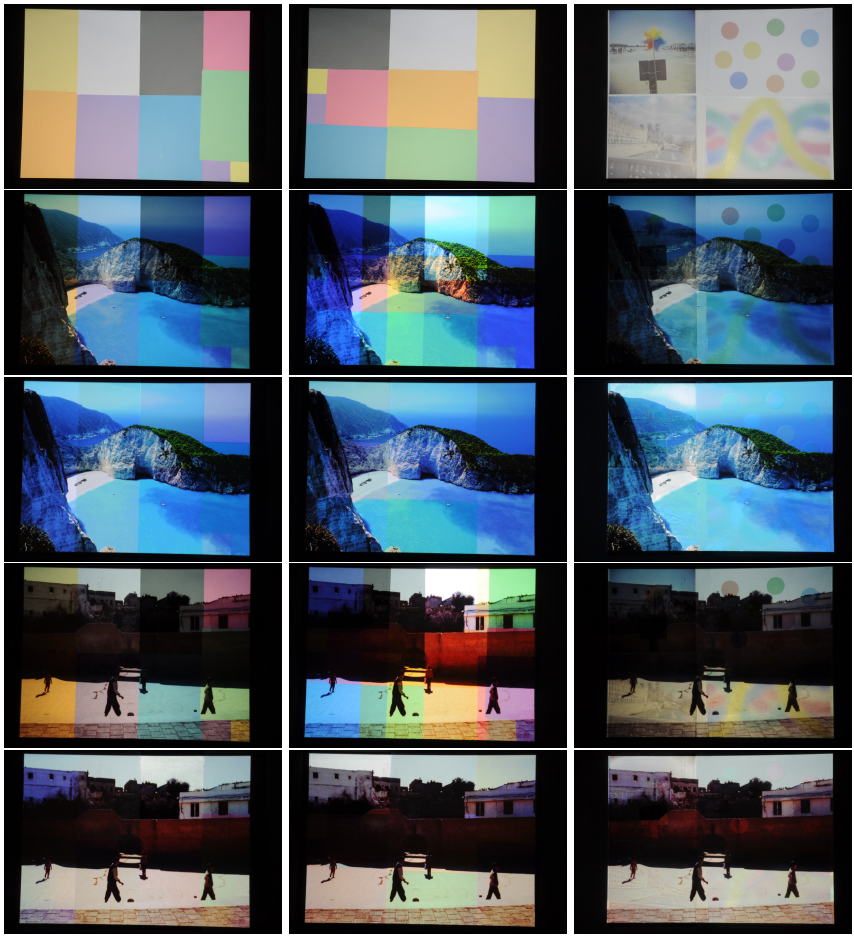

Fig. 4. From left to right: First row: The projection surface. Second row: Image 1 before compensation. Third row: Image 1 after compensation. Fourth row: Image 2 before compensation. Fifth row: Image 2 after compensation.

projector. This is illustrated in the second column of Fig. 4 (second and fourth row), where the projection surface has been changed while the compensation has

remained the same with the one of the first column. Finally, the robustness of the proposed method was tested on considerably complex surfaces with high spatial frequency that make the compensation extremely challenging. The results on such a surface are presented in the third column of Fig. 4.

4.3 Evaluation

In order to evaluate quantitatively the performance of the proposed method, the mean S-CIELAB color difference [19] between the compensated image projected on a colored surface and the reference image projected on a white surface was computed. This evaluation concerns image appearance. Hence, widely used measures such as RMSE, PSNR or even CIELAB differences are not appropriate since they do not take into account any spatial information. The evaluation results for a typical monitor (72 dpi) viewed at 18 inches are presented in Table 1.

It should be noted that the slight misalignement of the images due to small movements of the camera increases noticeably the color differences. However, the improvement using the proposed compensation is still visible.

Table 1. The mean S-CIELAB difference according to the desired appearance

	Image 1		Image 2	
	Non-compensated	Compensated	Non-compensated	Compensated
Surface 1	30.9	16.2	16.1	10.4
Surface 2	16.0	12.2	11.7	8.7
Surface 3	17.1	11.8	10.7	8.9

5 Conclusions

A novel method for the photometric compensation in a projector-camera system is proposed, which enables the projection on an arbitrary surface. More importantly, this new approach estimates the reflectance of the projection surface using a single input image and can be used for applications where the projection surface is dynamic such as in the case of a moving object. In contrast with previous attempts in dynamic environments, it can compensate for surfaces with vivid colors and high spatial frequencies that are easily perceived by the viewer. Future work will seek to implement it in a real time system for dynamic scenes in order to make real time compensation on humans and moving objects feasible. Moreover, the desired appearance match will be applied in a color appearance model so that the compensation can be driven by the human visual system instead of being driven by the capture of the camera, as it is currently made. Finally, the number and variety of colors used as the training set for the reflectance estimation will be further examined.

Acknowledgments. We thank Prof. Alain Trémeau and Ass. Prof. Damien Muselet (Laboratoire Hubert Curien, Université Jean Monnet) for hosting us and providing us access to the Minolta CS-1000 spectroradiometer.

References

1. Amano, T.: Projection based real-time material appearance manipulation. In: IEEE CVPR Workshops, pp. 918–923 (2013)
2. Amano, T., Kato, H.: Appearance control using projection with model predictive control. In: ICPR, pp. 2832–2835 (2010)
3. Ashdown, M., Okabe, T., Sato, I., Sato, Y.: Robust content-dependent photometric projector compensation. In: IEEE CVPR Workshops, pp. 6–6, June 2006
4. Bimber, O., Emmerling, A., Klemmer, T.: Embedded entertainment with smart projectors. Computer **38**(1), 48–55 (2005)
5. CIE TC 8–01: A color appearance model for color management systems. Publication 159. Vienna: CIE Central Bureau (2004)
6. Fujii, K., Grossberg, M., Nayar, S.: A projector-camera system with real-time photometric adaptation for dynamic environments. In: IEEE Computer Society CVPR. vol. 2, p. 1180, June 2005
7. Grossberg, M., Peri, H., Nayar, S., Belhumeur, P.: Making one object look like another: controlling appearance using a projector-camera system. In: IEEE Computer Society CVPR. vol. 1, pp. I-452–I-459 (2004)
8. Grundhofer, A.: Practical non-linear photometric projector compensation. In: IEEE CVPR Workshops, pp. 924–929, June 2013
9. Law, A.J., Aliaga, D.G., Sajadi, B., Majumder, A., Pizlo, Z.: Perceptually based appearance modification for compliant appearance editing. Computer Graphics Forum **30**(8), 2288–2300 (2011)
10. Luo, M.R.: Cie 2000 color difference formula: Ciede 2000. Proc. SPIE **4421**, 554–559 (2002)
11. McCamy, C.S., Marcus, H., Davidson, J.G.: A color-rendition chart. J. Appl. Photogr. Eng. **2**(3), 95–99 (1976)
12. Moreno, D., Taubin, G.: Simple, accurate, and robust projector-camera calibration. In: 3DIMPVT, pp. 464–471, October 2012
13. Nayar, S.K., Peri, H., Grossberg, M.D., Belhumeur, P.N.: A projection system with radiometric compensation for screen imperfections. In: IEEE International Workshop on Projector-Camera Systems (PROCAMS) (2003)
14. Ng, T.T., Pahwa, R.S., Bai, J., Tan, K.H., Ramamoorthi, R.: From the rendering equation to stratified light transport inversion. Int. J. Comput. Vision **96**(2), 235–251 (2012)
15. Park, H., Lee, M.H., Seo, B.K., Park, J.I., Jeong, M.S., Park, T.S., Lee, Y., Kim, S.R.: Simultaneous geometric and radiometric adaptation to dynamic surfaces with a mobile projector-camera system. IEEE Transactions on Circuits and Systems for Video Technology **18**(1), 110–115 (2008)
16. Seime, L., Hardeberg, J.Y.: Colorimetric characterization of lcd and dlp projection displays. Journal of the Society for Information Display **11**(2), 349–358 (2003)

17. Wetzstein, G., Bimber, O.: Radiometric compensation through inverse light transport. In: 15th Pacific Conference on Computer Graphics and Applications, pp. 391–399, October 2007
18. Xu, Y., Aliaga, D.G.: Robust pixel classification for 3d modeling with structured light. In: Proceedings of Graphics Interface 2007. GI 2007, pp. 233–240. ACM (2007)
19. Zhang, X., Silverstein, D., Farrell, J., Wandell, B.: Color image quality metric s-cielab and its application on halftone texture visibility. In: IEEE Proceedings of Compcon. pp. 44–48, February 1997